JOURNAL OF Materials CHEMISTRY

Synthesis in fluoride media and characterisation of aluminosilicate zeolite beta

Miguel A. Camblor,* Avelino Corma and Susana Valencia

Instituto de Tecnología Química (UPV-CSIC), Avda. Los Naranjos s/n, 46022-Valencia, Spain

Zeolite beta has been synthesised for the first time in a wide range of initial Al/(Al+Si) ratios (0–0.14) in the presence of F^- and TEA^+ at near neutral pH. The samples have been characterised by a number of techniques and compared to those synthesised in basic medium. An increase in crystal size and crystallinity as the Si/Al ratio increases together with an enhanced resolution of the XRD pattern and of the IR and ^{29}Si MAS NMR spectra are apparent. This is attributed to an enhanced local order as Si substitutes for Al in the zeolite framework. IR and ^{27}Al MAS NMR demonstrate dealumination is more severe the lower the Si/Al ratio. The presence of F^- in the as-made samples induces significant changes in the IR spectrum in the region of characteristic framework vibrations (500–650 cm^{-1}) probably due to a distortion of the framework. The determination of the micropore volume has been carried out using different methods, the t-plot method giving the more reliable results. Apparently, thermal analysis allows one to distinguish between TEA^+ cations compensating for F^- anions from those compensating for framework Al, as the latter appear to be oxidised at a higher temperature.

Introduction

The fluoride route to the synthesis of microporous materials is based on the substitution of OH^- anions, usually employed in the hydrothermal synthesis of these materials, by fluoride anions which may also play a mineralising role. This procedure was first used for the crystallisation of pure silica MFI[1] and also for the incorporation of Al and B into it.[2] From that point it has been extensively applied to several other zeolites, clathrasils, alumino- and gallo-phosphates.[3,4] Very recently, we have successfully applied the fluoride route to the synthesis of very low framework density pure silica polymorphs, namely pure silica beta,[5] ITQ-4[6] and ITQ-3.[7]

Zeolite beta is a large-pore and high-silica microporous material usually synthesised in basic medium in the presence of tetraethylammonium hydroxide and alkali metal cations.[8] This structure has been reported to be an intergrowth of two or more polymorphs[9,10] comprising a three-dimensional system of 12-membered ring channels. One of these polymorphs shows chirality and all these features make zeolite beta an attractive material from the catalytic point of view. The Si/Al molar ratio for zeolite beta described in the original patent is in the range 5–100[8] and important efforts have been carried out in order to exceed this limit. For almost 30 years it seemed to be not possible to obtain zeolite beta without Al or another T^{III} element. Very recently, the synthesis of pure silica or Ti-beta zeolite without Al was made possible by using deboronated or dealuminated zeolite beta seeds, respectively.[11,12] On the other side, Al-free Ti-beta synthesised in basic medium with 4,4′-trimethylenebis(*N*-benzyl-*N*-methylpiperidinium) as organic cation has also been reported.[13,14] However, we have recently reported the spontaneous nucleation and growth of pure silica and Ti-beta zeolites in the presence of tetraethylammonium cations and fluoride anions, at near neutral pH,[5,15,16] and the materials have been shown to be more hydrophobic[17] and free of connectivity defects compared to those synthesised in basic media. The synthesis of zeolite beta in a fluoride medium using 1,4-diazabicyclo[2.2.2]octane (DABCO) and methylamine as templates was previously reported.[18] However, the method was very limited because the Si/Al ratio was restricted to a very narrow range (Si/Al=9–22, compared to Si/Al=6.5 to pure silica in the method reported here) and the presence of seeds was necessary to obtain a fully crystallized material. It was reported there that no zeolite beta was obtained using other templates apart from DABCO in fluoride medium, in contrast to the results we present here.

As very recently reported, zeolite beta synthesised in F^- medium exhibits a higher hydrophobic character than the material synthesised in basic medium and this has been proved to have benefits for its catalytic activity and selectivity in reactions where molecules of different polar character are involved.[17,19] In the present work, we report on the synthesis of aluminosilicate zeolite beta in the presence of tetraethylammonium cations and fluoride anions at near neutral pH in a wide range of Si/Al ratios. The materials obtained have been characterised by using different techniques and compared to those synthesised in basic medium.

Experimental

The samples were obtained by hydrothermal synthesis at 140 °C in PTFE-lined stainless-steel autoclaves rotated at 60 rpm. Synthesis mixtures were prepared by hydrolysing tetraethylorthosilicate (TEOS) (98%, Merck) in an aqueous solution of tetraethylammonium hydroxide (TEAOH) (35%, Aldrich). Then a solution made by dissolving metal aluminium (99.95%, Merck) in aqueous TEAOH was added and the mixture was kept under stirring until the complete evaporation of the ethanol formed upon hydrolysis of TEOS (within the detection limit of ^1H NMR). Finally, hydrofluoric acid (48%, Merck) and, optionally, zeolite beta seeds were added. When used, zeolite beta seeds were prepared from a gel of composition SiO_2 : 0.04 Al : 0.56 TEAOH : 6.5 H_2O crystallised at 140 °C for 72 h, yielding nanocrystalline zeolite beta with *ca.* 50 nm average crystal size and Si/Al=21.[20] Chemical composition of the synthesis mixtures crystallised as shown above can be expressed as follows:

$$SiO_2 : xAl_2O_3 : (0.54+2x)TEAOH : (7+2x)H_2O : (0.54+2x)HF$$

x being varied between 0 and 0.167. This corresponds to the final composition, *i.e.* water evaporated during removal of ethanol as well as water consumed in the hydrolysis of TEOS (two H_2O molecules per TEOS) have been subtracted.

After the required crystallisation time, the autoclaves were cooled down to room temperature. The pH of the mother liquors was in the range 8–9.5. The products were filtered and washed extensively with deionised water. Finally, the samples were calcined at 580 °C in static air for 3 h in order to remove

the organic molecules and fluoride anions occluded in the solids.

Crystallinity and phase purity of the materials were determined by powder X-ray diffraction (XRD) in a Philips PW1830 diffractometer with Cu-Kα radiation, the crystallinity being defined as the ratio of peak areas under the most intense peak ($2\theta = 22.4^\circ$) for each sample and for a highly crystalline standard sample synthesised in basic medium. IR spectroscopy was also used to characterise the samples in a Nicolet 710 FTIR spectrometer using KBr wafers for the framework vibrations region and self-supported wafers for the OH region. Pyridine adsorption experiments and desorption at different temperatures were performed and monitored by IR spectroscopy in order to study the acidity. For this, the samples were outgassed overnight at 400 °C, then 1866 Pa of pyridine were introduced and desorption was carried out successively at 250, 350 and 400 °C.

Thermogravimetric and differential thermal analyses (TGA–DTA) were performed in a Netzsch STA 409 EP thermal analyser with about 20 mg of sample and a heating rate of 10 °C min^{-1} in air flow (6 l h^{-1}). ^{29}Si MAS NMR spectra were recorded on a Varian VXR 400S WB spectrometer at a ^{29}Si frequency of 79.459 MHz and a spinning rate of 5 kHz with a 73.6° pulse length of 3.0 μs and a recycle time of 60 s. The ^{29}Si chemical shifts are reported relative to TMS. ^{27}Al MAS NMR spectra were recorded on the same spectrometer at a ^{27}Al frequency of 104.214 MHz and a spinning rate of 7 kHz with a 10° pulse length of 0.5 μs and a recycle delay of 0.5 s. The ^{27}Al chemical shifts are reported relative to an $Al(H_2O)_6^{3+}$ solution.

Chemical composition was determined by atomic absorption in a Varian SpectrAA-10 Plus (Al) and elemental analysis in a Fisons EA1108CHN-S (C, H, N). Si was determined by difference. Fluoride content was measured using an ion-selective electrode after dissolution of the samples.[21] Scanning electron microscopy in a JEOL 6300 microscope was used in order to know the size and morphology of the crystals. Nitrogen and argon adsorption experiments at 77 and 85 K, respectively, were carried out in a Micromeritics ASAP 2000.

Results and Discussion

Synthesis

Under the synthesis conditions described above it was possible to obtain highly crystalline zeolite beta in a range of initial Al/(Al + Si) ratios comprised between 0 and 0.14, as can be seen in Table 1. In this range, no impurities were detected, so it can be concluded that in these conditions zeolite beta is easily obtained from pure silica and aluminosilicate gels containing TEA cations and fluoride anions at near neutral pH. It has to be pointed out that the presence of seed crystals is not necessary in this system to obtain zeolite beta and this can spontaneously nucleate and grow from high Al-containing gels to pure silica ones, in contrast to the reported synthesis using fluoride, DABCO and methylamine.[18] It is also remarkable that the materials obtained with this method are highly stable at the synthesis conditions and once the maximum crystallinity has been reached, the zeolite yield and crystallinity are maintained for at least 10 additional days.

An interesting feature of this synthesis procedure is that the yield of crystalline solids is always about 90–100% (see Table 1). This is a significant improvement compared to the conventional synthesis in basic medium where the yield of solids decreases as the Si/Al ratio increases due to a decreased efficiency of Si incorporation.[20,22] The crystallisation time necessary to obtain zeolite beta increases considerably as the amount of Al in the synthesis mixture increases, as can be observed in Table 1, where it is shown that the gel with the lowest Si/Al ratio requires 62 days of heating for its complete crystallisation. This dependency of the crystallization time on the Al content has also been observed for zeolite beta synthesised in basic medium in the absence of alkali metal cations.[20]

It can also be observed in Table 1 that Al incorporation into the zeolite is about 85–100% for samples with Si/Al ratios >10, so the Si/Al ratio in the solid is quite similar to that in the synthesis mixture. However, for crystalline solids with lower Si/Al ratios, Al incorporation becomes $<80\%$ and the samples present higher Si/Al ratios than those in the gel. This is possibly related to the limit of Al incorporation to the zeolite due to the requirement of counterbalancing the negative charge introduced by Al. This is restricted to about 7–8 atoms, possibly less, per unit cell as this is the maximum number of organic molecules which can be accommodated in the channels and no alkali metal cations are involved in the synthesis. As can be seen in Table 1, the sample with Si/Al = 6 in the starting mixture contains 7.8 Al/u.c. while there are only 6.5 TEA cations as measured by elemental analysis. This result could indicate that in the as-made material not all the Al is incorporated in the zeolite framework in this sample (see below). An interesting result is also shown in Table 1 for an experiment with Si/Al = 7 in the starting mixture and a slightly higher amount of F^- anions [HF/(Si + Al) = 0.60 instead of 0.54]. In this experiment the zeolite beta obtained exhibits only 64% Al incorporation. This is possibly related to the high stability of the aluminium fluoride complexes and has also been observed for MFI zeolite synthesised in fluoride medium, where high degrees of Al, B or Ga incorporation requires F^-/Si ratios as small as possible.[2,23,24]

Table 1 Synthesis results in the crystallisation of zeolite beta samples in fluoride medium and in the absence of seeds

Si/Al in gel	synthesis time/ days	crystallinity (%)	yield of solids[a] (%)	Si/Al in solid[b]	Al/u.c.	Al incorporation (%)
∞	1.6	110	98	∞	—	—
200	9.5	104	89	212	0.3	84
100	5.7	104	92	100	0.6	90
50	6.7	101	90	49	1.3	92
25	0.6	8	90	—	—	—
25	2.6	97	91	25	2.4	93
12.5	2.7	11	94	—	—	—
12.5	5.7	105	91	11.8	5.0	96
8	28	101	89	9.1	6.4	80
7	17	15	92	7.3	—	—
7	52	105	94	8.9	6.5	76
7[c]	21	106	89	10.0	5.8	64
6	27	0	90	6.9	—	—
6	62	97	86[d]	7.2	7.8	74

[a]Calculated in calcined samples with respect to $SiO_2 + Al_2O_3$ in the starting mixture. [b]Measured by chemical analysis. [c]HF/(Si + Al) = 0.60. [d]Some solid loss upon filtration occurred.

As the Al content in the zeolite increases the amount of fluoride anions incorporated should decrease because the charge of TEA cations is balanced by the negative charge introduced by Al in the framework. Chemical analysis of samples with different Al content shows a decrease in the amount of fluoride in the solid as the Al content increases until a value of 4–5 Al/u.c., above which it remains constant or slightly increases (Fig. 1). This increase in the fluoride content is accompanied by an increase in the amount of TEA cations which could suggest the presence of some kind of TEA oxofluoroaluminate complexes in the samples with high Al content.

The efficiency of this synthesis method is clearly related to the presence of fluoride anions. However, the F^- method was employed before for zeolite beta synthesis[18] but a much lower range of Si/Al ratios was observed and the presence of seeds was necessary to obtain good crystallinity samples. In addition, no zeolite beta crystallised in fluoride medium in those conditions with other templates different from DABCO. The possible explanation is that our synthesis procedure is based on low H_2O/SiO_2 and F^-/SiO_2 ratios and relatively low temperatures, in contrast to those reported by other authors, and we have observed that in such conditions the formation of pure silica zeolite beta is favoured, as will be discussed elsewhere.[25] The use of F^- anions at low H_2O/SiO_2 and F^-/SiO_2 ratios has led to the synthesis of three silica materials which, together with ITQ-1[26] (synthesised in basic medium), show the lowest framework density ever reported for pure silica materials, *i.e.* pure silica beta,[5] ITQ-3[7] and ITQ-4[6] (with framework densities of 15.5, 16.3 and 17.0 $SiO_2/1000$ Å^3, respectively) and gives the opportunity to extend the use of this method to synthesise new microporous materials with lower density.

X-Ray diffraction

X-Ray diffraction patterns of the final solids show the typical features of zeolite beta with sharp and broad reflections characteristic of an intergrowth of different polymorphs. It is remarkable that no other crystalline phases were observed competing with beta and the samples usually exhibit >100% crystallinity when referred to a standard highly crystalline sample synthesised in basic medium. We attribute the enhanced crystallinity of these samples to the decrease in connectivity defects (see below). It has to be pointed out that the resolution of the X-ray diffraction patterns improves as the Si/Al ratio increases, as can be seen in Fig. 2. This is not an effect of different crystallinities since both samples presented in this figure exhibit >100% crystallinity, and is possibly due to Al incorporation in the framework which reduces the degree of order. The resolution of the X-ray diffraction pattern of the sample with Si/Al = 200 looks very similar to that observed in pure silica zeolite beta.[5] As explained above, the sharpness and resolution of that pattern, compared to the standard one, is not only a consequence of the relatively large crystal size (0.5–5 μm), but is also due to the absence of connectivity defects which makes possible some fine features of the calculated XRD pattern for the proposed model to appear.[9] Those features (see arrows in Fig. 2) are not observable in high silica samples synthesised in basic media that usually present a high concentration of connectivity defects. In fact, the features in the low angle peak could suggest that this sample could have a different fault probability and may be nearer polymorph A than the standard samples.[5]

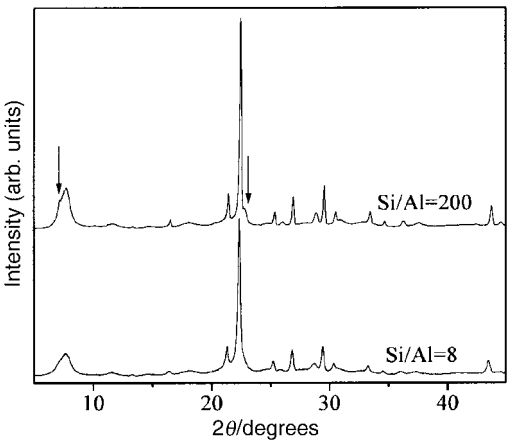

Fig. 2 X-Ray diffraction patterns of samples synthesised in fluoride medium in the absence of seeds starting from different Si/Al ratios

An interesting property of these materials is their enhanced thermal stability. Concerning the stability upon calcination at 580 °C for 3 h in static air, samples obtained by the F^- method maintain their crystallinity better than those synthesised in basic medium, as can be observed in Fig. 3. In the figure it is also shown that, as the Al content increases, the crystallinity loss upon calcination becomes bigger and the crystallinity of the as-made samples also decreases. This can be an effect of the higher Al content which makes the zeolite framework easier to be damaged in the calcination process. Nevertheless there is a big difference between these samples and those synthesised at high pH which exhibit a maximum in crystallinity for about 4 Al/u.c., the rest of the samples being around 60–65% crystalline after calcination. The larger difference between both series corresponds to samples with low Al

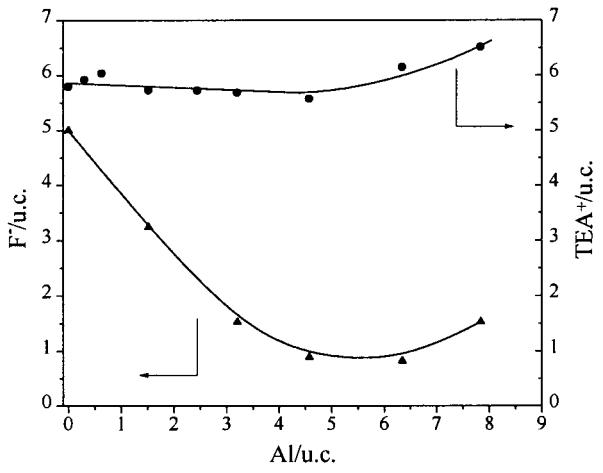

Fig. 1 Variation of the TEA^+ (●) and F^- (▲) content in zeolite beta samples as a function of the Al content

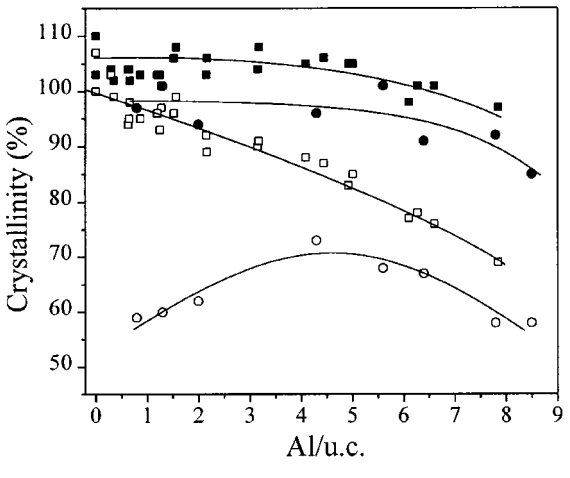

Fig. 3 Crystallinity of as-made (filled symbols) and calcined samples (open symbols) of zeolite beta synthesised in fluoride (■,□) and in basic medium (●,○)

content and can be related to the absence of connectivity defects in the high-silica materials synthesised by the F^- method and their presence in samples obtained in basic medium, together with the smaller crystal size in the latter. As the Al content increases beyond 4 Al/u.c. the differences between both series of samples become smaller but still significant (*ca.* 10% crystallinity) which is possibly due to the fact that samples synthesised in basic medium usually contain more connectivity defects than the amount necessary to counterbalance the positive charge introduced by the organic cations.[11,27]

IR spectroscopy

The IR spectra of the as-made materials in the framework vibration region are shown in Fig. 4. In the 500–650 cm^{-1} region characteristic vibrations of the zeolite structure appear and show notable differences as the Al content increases. The sample with the highest Si/Al ratio show several overlapping bands and as the Al content increases fewer, well defined bands appear in the typical positions of zeolite beta. We attribute this effect to the incorporation of F^- in the zeolite which can influence the vibrations of the T atoms, as F^- is usually located in small cages within the zeolite framework[28–31] possibly modifying T—O—T angles. Furthermore, coordination of F^- to framework Si giving rise to pentacoordinated $[SiO_{4/2}F]^-$ has been recently demonstrated,[32,33] and could be a general feature of zeolites synthesised in fluoride media. This would certainly affect the IR framework vibration. As the Al content increases the amount of F^- in the zeolite decreases (see above) and the spectrum becomes more like that of zeolite beta synthesised in basic media.

The IR spectra of the calcined samples in this region (Fig. 5) exhibit bands in the characteristic positions of zeolite beta. Note that the sample with Si/Al = 212 displays now an IR spectrum very similar, though better resolved, to the low silica samples, in contrast to the observation in the as-made materials (Fig. 4). This gives support to our conclusion on the effect of F^- on the IR spectrum. Another remarkable feature is the lack of a band at about 960 cm^{-1} typical of Si—OH vibrations which confirms the absence of a significant concentration of connectivity defects. This band is present in high silica samples synthesised in OH^- medium (Fig. 5). Only a weak shoulder is observed for the calcined samples with low Si/Al ratios which is assigned to Si—OH groups generated upon calcination of the material due to dealumination processes, with possibly a contribution of external Si—OH groups because of the decrease in crystal size as the Al content increases (see below).

The acidic properties of the calcined materials have been studied by adsorbing pyridine as a basic probe molecule, desorbing at different temperatures and following the process

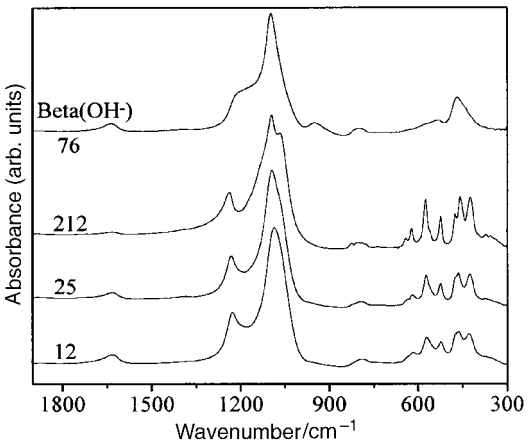

Fig. 5 IR spectra in the framework vibration region of calcined samples with different Si/Al ratios. One sample synthesised in basic medium has been also included.

by IR spectroscopy. IR spectra in the OH stretching region for samples with different Si/Al ratios after being outgassed at 400 °C are shown in Fig. 6. The intensity of the band around 3610 cm^{-1} assigned to bridging hydroxyl groups associated with Al in the zeolite (Brönsted acid sites) exhibits a maximum for samples containing about 2–3 Al/u.c. This indicates that dealumination processes occurring during calcination are more severe in samples with high Al content. After pyridine adsorption this band disappears and the bands associated with the pyridinium ion adsorbed in Brönsted acid sites (*ca.* 1545 cm^{-1}) and pyridine coordinated to Lewis sites (*ca.* 1450 cm^{-1}) appear. Desorption at different temperatures gives information about the acid strength of the sites. The intensity area of these bands in arbitrary units is represented in Fig. 7 as a function of the Al content of the samples for different desorption temperatures. The figure shows a maximum in the amount of Brönsted acid sites retaining pyridine at 250 and 350 °C for samples with about 3–4 Al atoms per unit cell. In the case of the strongest sites (desorption at 400 °C) there is a great dispersion probably due to the low intensity of the band. These results can be interpreted considering an enhanced dealumination as the Al content increases, producing a maximum in acidity for samples with intermediate Si/Al ratios (15–20). Moreover, the probable presence of TEA oxofluoroaluminate complexes in samples with more than 4–5 Al/u.c. could also have an effect in the decrease of acidity (see above). The figure also shows, despite the large dispersion of the points, an increasing trend in the amount of Lewis acid sites when increasing the Al content which agrees with dealumination processes increasing in this

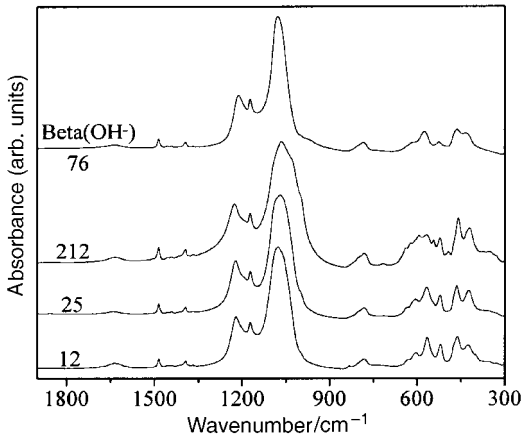

Fig. 4 Infrared spectra in the framework vibration region of as-made zeolite beta samples with different Si/Al ratios. One sample synthesised in basic medium has been included for comparison.

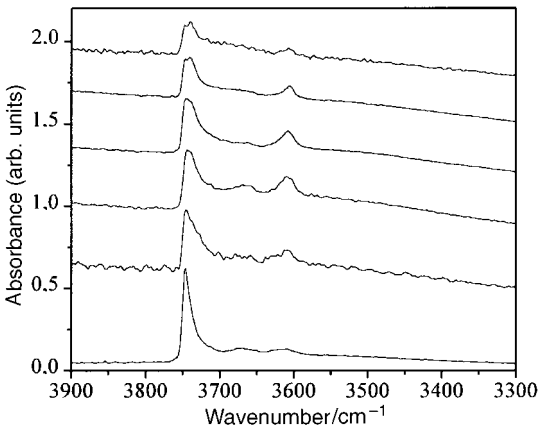

Fig. 6 Infrared spectra in the OH stretching region of calcined zeolite beta materials with different Al content: (bottom to top) 6.21, 4.92, 3.20, 2.17, 1.25 and 0.65 Al/u.c.

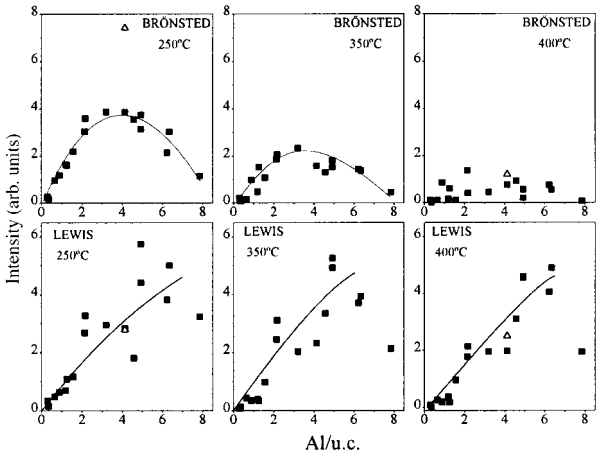

Fig. 7 Intensity of the bands appearing in the IR spectra corresponding to pyridine adsorbed in Brönsted and Lewis acid sites in calcined zeolite beta samples with different Al content. The symbol (△) corresponds to a zeolite calcined in N_2 flow followed by air flow while the remainder of the samples were calcined in static air.

direction. Nevertheless, Al-rich samples show a decrease in the amount of Lewis acid sites as well as in the Brönsted acid sites which suggest the presence of non-acidic polycondensed alumina or silica-alumina extraframework species generated during calcination, although the presence of TEA oxofluoro complexes in the as-made materials can also contribute to this result.

An interesting result is that obtained for the sample with 4.1 Al/u.c. calcined in N_2 flow followed by air compared to calcination in static air. This sample exhibits a much higher intensity in the band associated with Brönsted acid sites retaining pyridine at 250 °C while there are minor differences in the number of the strongest sites (desorption at 400 °C) as compared to the sample calcined in standard conditions. This indicates a lower dealumination degree upon calcination in N_2/air which has also been observed in nanocrystalline zeolite beta synthesised in basic medium.[34] However, there are no significant differences in the number of Brönsted or Lewis acid sites retaining pyridine at 400 °C. Apparently, calcination in N_2/air improves the stability of the Al related to the less acidic sites.

Scanning electron microscopy

Zeolite beta synthesised in basic medium typically yields small crystallites, usually <1 μm[35] and, when the synthesis is carried out in the absence of alkali cations, nanocrystals as small as 10 nm can be obtained.[20] On the other side, syntheses carried out in F^- medium typically produce bigger crystals which has been related to the lower mineralising power of F^- as compared to OH^- causing lower supersaturation and smaller nucleation rates.[2] In the samples obtained by this synthesis procedure we observe larger crystals than those synthesised in basic medium. When the crystals are large enough they show the truncated square bipyramidal morphology typical of zeolite beta. SEM images are displayed in Fig. 8 and a decrease in crystal size when increasing the Al content in the sample can be observed from *ca.* 3 μm for Si/Al = 212 to <1 μm for Si/Al = 9. This has also been observed for zeolite beta synthesised in basic medium in the absence of alkali metal cations[20] which also shows a longer synthesis time for lower Si/Al ratios. Apparently, as the Al content increases the ratio of the nucleation rate to the crystal growth rate increases.

It has to be remarked that the crystal size is an important parameter in catalysis and, when diffusional problems can exist, it is convenient to use small crystal size catalysts. For this reason, we performed syntheses of these materials using zeolite beta seed crystals with very small crystal size (*ca.* 50 nm). The zeolite beta produced had a smaller crystal size, usually <0.5 μm. Fig. 8(a) and (b) show the difference in crystal size for materials obtained from starting synthesis mixtures with Si/Al = 200 in the presence and the absence of seeds, respectively. The unseeded mixture gives zeolite beta with an average crystal size around 3 μm and the seeded one produces crystal sizes lower than 0.2 μm.

N_2 and Ar adsorption experiments

N_2 and Ar adsorption isotherms were used in order to measure the micropore volume of the calcined zeolites with different Si/Al ratios. The corresponding N_2 adsorption isotherms are presented in Fig. 9 and those obtained with Ar (not shown) are very similar. In the isotherms there is an increase in the slope of the curve for intermediate relative pressures in zeolites with more than 5 Al/u.c. which can be due to the existence of mesopores in the samples (see below). The micropore volume in zeolites is calculated in the literature by different procedures: from the t-plot method,[36] from the adsorbed volume at a given relative pressure (normally $P/P_0 = 0.3$) and from the extrapolation to $P/P_0 = 0$ of the slope of the isotherm in the plateau.

The results obtained using the t-plot method are shown in Fig. 10(a) where a similar variation of the N_2 and Ar adsorption data with the Al content of the zeolite can be observed. There is a slight initial increase until 3–4 Al/u.c. and a subsequent decrease in the micropore volume for high Al-containing samples. The initial increase could be explained considering the generation of connectivity defects in dealumination processes during calcination which could open up small cages contained in the zeolite beta structure ([4^3 5^4] and [4^2 5^4 6^2] cages) making them accessible to N_2 and Ar. On the other hand, the decrease in micropore volume for higher Al contents could be due to the decrease in crystallinity after calcination (see Fig. 3) and also to the creation of mesopores by destruction of large portions of the structure which would decrease the micropore volume. The possibility of blockage of the channels by extraframework species has to be ruled out since this is not likely to occur in a three-dimensional large pore channel system. Finally, the effect of nanocrystallinity in this parameter has to be taken into account as shown elsewhere.[34] However, the differences are not as pronounced as those obtained for nanocrystalline zeolite beta and in these samples it is not easy to determine the crystal size from the SEM pictures owing to agglomeration of the crystallites.

When the micropore volume is obtained from the adsorbed volume at a relative pressure of $P/P_0 = 0.3$, the trend observed from the N_2 isotherm differs from that of the Ar isotherm [Fig. 10(b)]. The results of N_2 adsorption exhibit an initial increase until about 3 Al/u.c. and then a plateau. The increase could be explained by the opening of the small cages, as commented above. However, this increase is too large and probably this method overestimates the micropore volume since if the isotherm is not flat at $P/P_0 = 0.3$ adsorption in small mesopores already occurs at this relative pressure. On the other side, from the Ar isotherms a maximum in the micropore volume is obtained at about 3 Al/u.c. which could suggest that at this relative pressure Ar is not yet being adsorbed in the mesopores.

Finally, if the micropore volume is calculated from the extrapolation to zero of the slope of the isotherm in the plateau similar trends to those observed from the t-plot are observed, though higher values of the micropore volume and a larger slope in the increasing part are obtained [Fig. 10(c)]. From these results it can be concluded that the method used to determine the micropore volume greatly influences the values obtained which makes it difficult to compare values reported in the literature. For example, micropore volumes around 0.26–0.28 cm^3 g^{-1} are typically reported for zeolite beta and agree well with the values obtained in this work using the last two methods [Fig. 10(b) and (c)] on the N_2 isotherms of zeolite

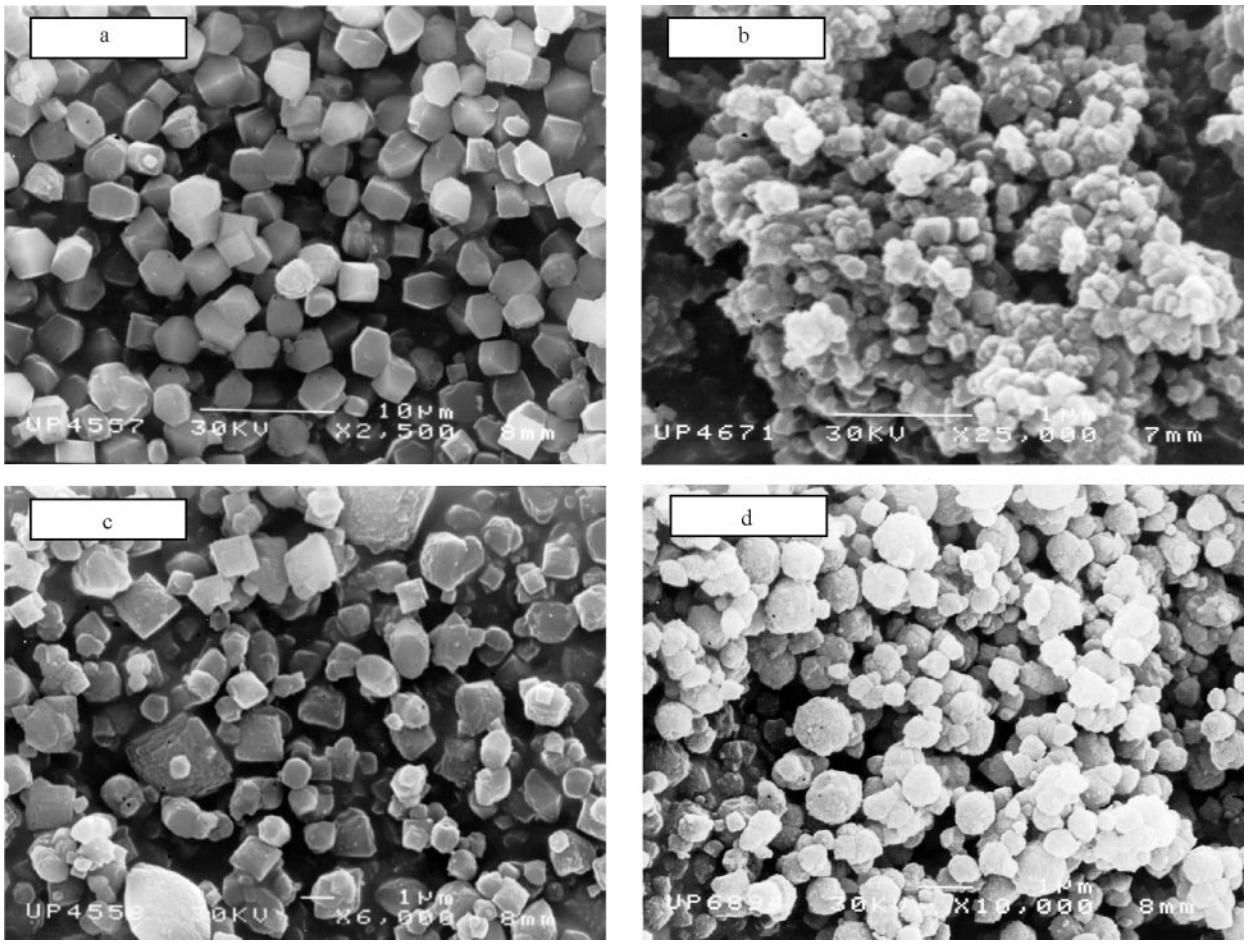

Fig. 8 SEM images of zeolite beta samples synthesised from different Si/Al ratios. (a) Si/Al = 200, (b) Si/Al = 200 (in the presence of seeds), (c) Si/Al = 25, (d) Si/Al = 8. Scale bar is 10 μm in (a) and 1 μm in (b)–(d).

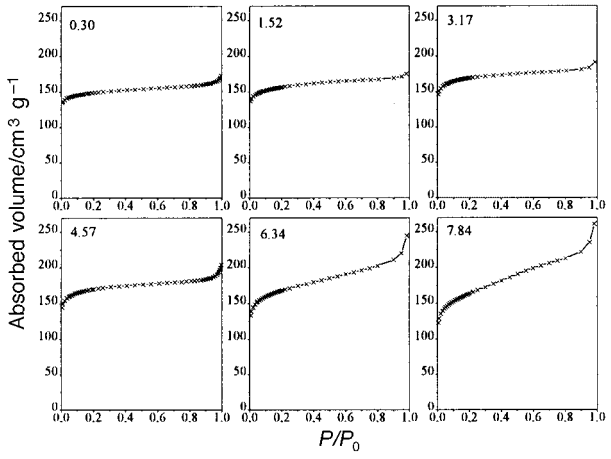

Fig. 9 N_2 adsorption isotherms of calcined zeolites with different Al content per unit cell

beta with 3–4 Al/u.c. However, by using these methods in the case of nanocrystalline zeolite beta too large values are obtained (>0.3 cm^3 g^{-1}) which can not be real and indicate that part of the mesopore volume is being measured as micropores. Therefore the t-plot seems to be the most suitable method for calculating micropore volumes and only if the isotherm is flat do the other measurements give similar results.

^{29}Si MAS NMR spectroscopy

We have previously reported the ^{29}Si MAS NMR spectrum of the calcined pure silica material obtained following the same synthesis procedure in the absence of Al.[5] This spectrum evidenced the absence of connectivity defects and exhibited only the resonance lines corresponding to Si(4Si) species occupying different crystallographic sites.[5] ^{29}Si MAS NMR spectra of the calcined samples displayed in Fig. 11 show a significant broadening of the bands as the amount of Al in the zeolite increases resulting in a significant loss of resolution. Samples with high Al contents exhibit ^{29}Si MAS NMR spectra quite similar to those reported for samples synthesised in basic media,[37,38] showing bands at around δ −116, −111, −104 and even at δ −95 for samples with 4.9, 6.2 and 7.8 Al/u.c. The lines at δ −116 and −111 correspond to Si(4Si) species, the third band can be due to both Si(3Si, 1Al) and Si(3Si, 1OH), making it impossible to determine accurately the framework Si/Al ratio from the spectra, and the last band is assigned to Si(2Si, 2Al) and/or Si(2Si, 2OH).

The loss of resolution when increasing the amount of Al has been observed in samples synthesised in basic media[38] and also when Ti is incorporated in the pure silica material.[17] The decreased resolution in the spectra can be attributed to the presence of connectivity defects generated by dealumination during the calcination, such processes being more severe as the Al content increases. Another contribution to the line broadening is the decreased local order caused by the incorporation of Al. As can be observed in Fig. 11 there is also a low field shift in the line position upon increasing the Al content which could suggest a diminution in the T—O—T angles. Assuming that no connectivity defects are present in the calcined samples and consequently the band appearing between δ −100 and −106 is due only to Si(3Si, 1Al) resonances, the Si/Al ratios calculated from the spectra are lower than those obtained from the chemical analyses. This result confirms the presence of defects generated in dealumination processes in the calcined zeolites. In the as-made materials the Si/Al ratio

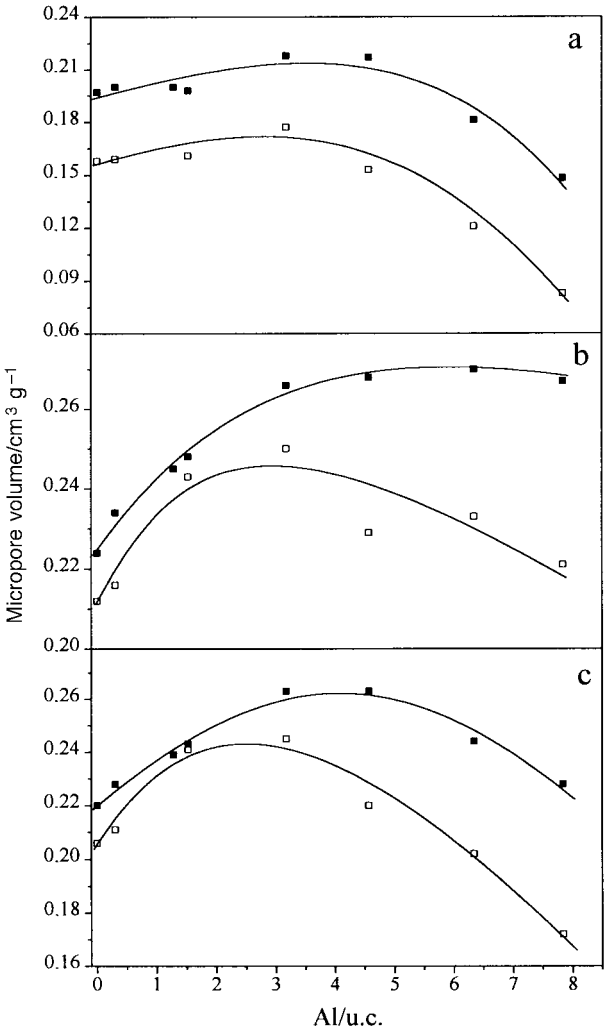

Fig. 10 Micropore volume of calcined zeolites obtained from the N_2 (■) and Ar (□) adsorption isotherms employing the t-plot method (a), calculated as the adsorbed volume at $P/P_0=0.3$ (b) and obtained from the extrapolation to $P/P_0=0$ of the slope of the isotherm in the plateau (c).

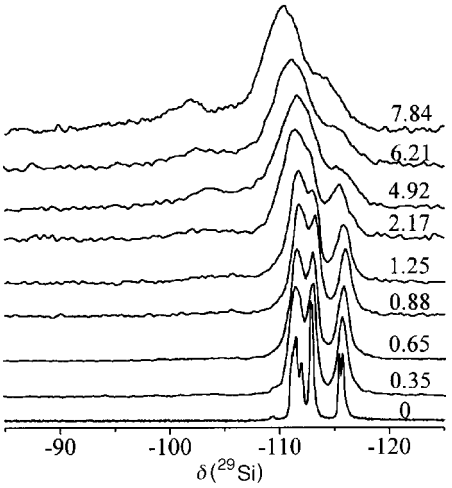

Fig. 11 ^{29}Si MAS NMR spectra of calcined zeolite beta materials with the Al content per unit cell shown near each trace

could also be calculated from the NMR spectra since the concentration of structural defects is expected to be very low. This calculation has been done in the samples with the highest Al content considering the known chemical shift ranges for Si[(4−*n*)Si, *n*Al] species and the results presented in Table 2

Table 2 Framework Si/Al ratio derived from ^{29}Si MAS NMR spectroscopy in as-made zeolite beta samples obtained in fluoride medium[a]

$(Si/Al)_{C.A.}$	$(Si/Al)_{NMR}$	Al/u.c. (C.A.)	Al/u.c. (NMR)
9.3	8.5	6.2	6.7
7.2	8.7	7.8	6.6

[a]C.A.: from chemical analysis. NMR: from ^{29}Si MAS NMR spectroscopy.

show that the amount of Al in the framework obtained from the NMR spectra in the zeolite with Si/Al=9.3 (6.7 Al/u.c.) is quite similar to that calculated from the chemical analysis (6.2 Al/u.c.). On the other hand, the Al content in the framework for the Al-richest sample differs from that of the chemical analysis by >1 Al/u.c. This result evidences that not all the Al is incorporated in the framework, as was suggested by the charge balance and the increasing TEA^+ and F^- content in this sample (see above).

^{27}Al MAS NMR spectroscopy

The spectra of the as-made zeolites (not shown) reveal the presence of a unique resonance with a centre of gravity in the δ 53.7–52.3 chemical shift range usually assigned to Al in tetrahedral coordination. No signals corresponding to Al in other environments are observed even for the sample with the highest Al content for which the chemical analysis showed a higher amount of Al than TEA^+ cations. This suggests the presence of either extraframework tetrahedral Al species with O, OH and/or F as ligands or very distorted and heterogeneous octahedral species producing very broad bands not detected in the spectrum[39] (invisible Al).

In the calcined zeolites the ^{27}Al MAS NMR spectra (Fig. 12) show the appearance of an additional band around δ 0 due to octahedral Al species besides that corresponding to tetrahedral Al in the range δ 55.0–51.5. The presence of octahedral Al could be attributed to extraframework Al species generated during calcination although the reversible transformation of octahedral Al to tetrahedral Al has been also proposed for zeolite beta.[40] In the samples with high Al content a broad band in the range δ −10 to −20 is also observed which would correspond to octahedral Al in very asymmetric and heterogeneous environments. On the other side, in the sample with the lowest Al content the band corresponding to tetrahedral Al is very asymmetric and even suggests the presence of two signals. Nevertheless, this could possibly be due to quadrupolar

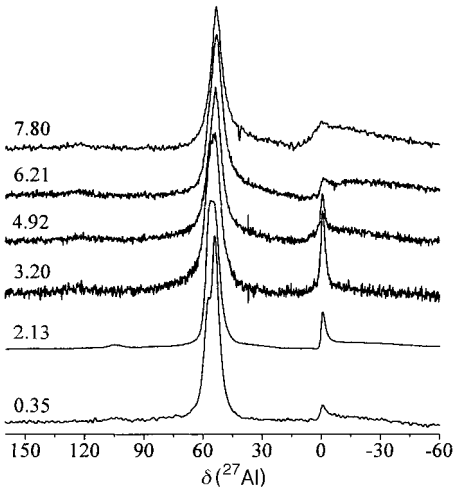

Fig. 12 ^{27}Al MAS NMR spectra of calcined samples with the Al content per unit cell shown near each trace

interaction and not necessarily to partial resolution of different crystallographic sites, as suggested previously.[38]

Thermal analysis

Thermogravimetric and differential thermal analyses were performed in order to determine the amount and nature of organic material filling the pores. The C/N ratio obtained from the elemental analyses (close to 8) and the ^{13}C MAS NMR spectra confirms the presence of TEA^+ cations in all the samples. As was indicated above when increasing the Al content in the zeolite up to 4–5 Al/u.c. the amount of F^- anions incorporated decreases owing to charge balance effects. As TEA^+ cations compensating for either F^- or framework Al charges can have different degradation temperatures, discrimination of both types of species by thermal analysis can be attempted. The TGA–DTA curves corresponding to samples with different Si/Al ratio are presented in Fig. 13 and show a first endothermic weight loss between 100 and 150 °C. Then a second step between 200 and 400 °C appears to be comprised of an endothermic peak, which is only observed for intermediate Si/Al ratios, and an exothermic more intense one. At about 450 °C another exothermic weight loss is observed and finally above 500 °C there is another exothermic weight loss which increases in intensity with the Al content in the sample.

The first endothermic weight loss is due to the desorption of occluded water and decreases in intensity as the Si/Al ratio increases which is consistent with a high hydrophobic character in the zeolites with low Al content. We assign the second step comprised of an endothermic peak followed by an exothermic one (200–400 °C) to decomposition of TEA^+ balancing F^- anions and oxidation of the products. On the other side, the exothermic weight losses around 450 and 600 °C are assigned to TEA^+ balancing framework Al charges, with the last step due to oxidation of products arising from incomplete oxidation or pyrolysis in the former steps. The basis for these assignments lay on the decreasing intensity of the lower temperature weight losses and the increase in the high temperature weight losses which are coincident with the decrease in fluoride content as the amount of Al increases. Moreover, in nanocrystalline zeolite beta synthesised in basic media TEA^+ cations balancing framework Al charges are burned off around 400–450 °C[34] and the TGA–DTA curves for the samples with low Si/Al ratio are similar to those obtained in the zeolite with high Al content synthesised in the fluoride medium [Fig. 13(c)].

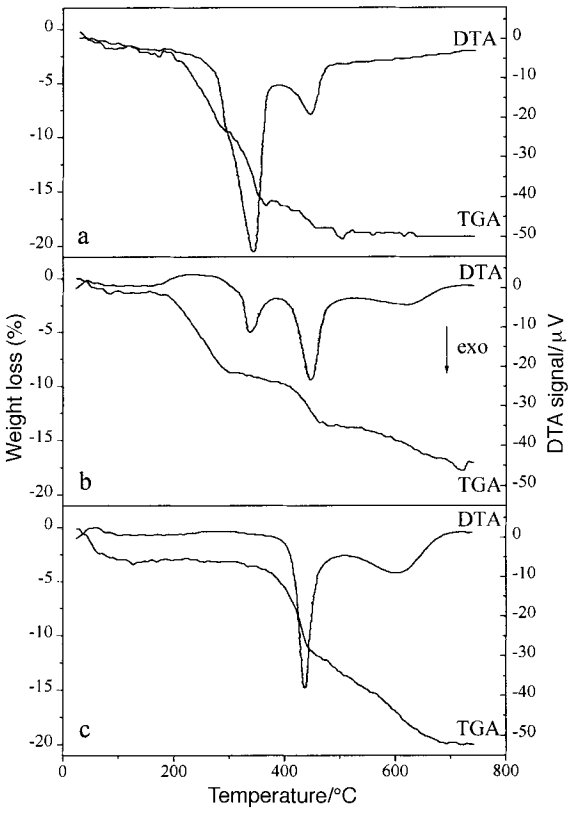

Fig. 13 TGA–DTA curves of zeolites beta with different Si/Al ratio: (a) Si/Al = 73, (b) Si/Al = 29, (c) Si/Al = 9.3

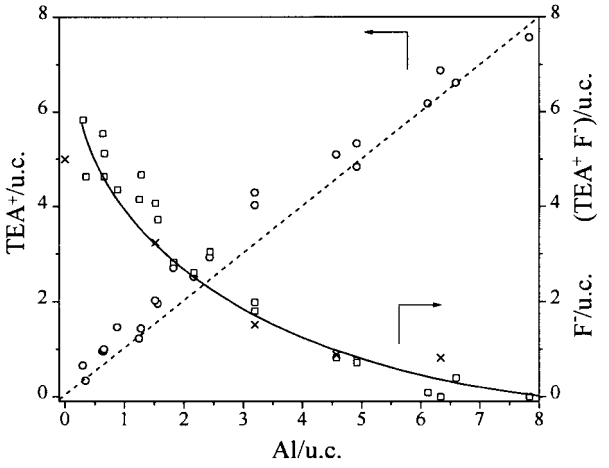

Fig. 14 Variation of the amount of TEA^+ cations compensating for F^- (□) or for framework Al (○) and F^- content obtained from the chemical analysis. The amount of TEA^+ has been calculated from the weight losses between 200 and 400 °C (□) and above 400 °C (○) observed in the TGA curves.

In order to confirm the above assignments the weight losses of the last (above 400 °C) and intermediate (between 200 and 400 °C) steps (expressed as TEA^+/u.c. and TEA^+F^-/u.c.) have been plotted as a function of the Al content in Fig. 14. As can be observed there is a good one-to-one correlation between the last weight loss and the amount of Al in the sample while the weight loss assigned to TEA^+ balancing F^- decreases with the Al content in the same way as the amount of F^- obtained from the chemical analysis. Therefore, these results seem to confirm the above assignments and could suggest a stronger interaction between the organic cations and framework Al than between the cations and fluoride. This has also been reported for MFI synthesised in fluoride medium where TPA^+ cations balancing the trivalent elements decompose at higher temperature than those balancing fluoride.[41,42] Nevertheless, another plausible explanation could be that nucleophilic F^- could attack the organic cations and favour its decomposition, which would be followed by combustion of the degradation products (triethylamine and ethylene). This would explain the observation that between 200 and 400 °C there are two overlapping processes, the first endothermic and the second exothermic.

Conclusions

The synthesis of zeolite beta carried out in a fluoride medium in the presence of TEA cations at near neutral pH has been achieved for the first time over a very wide range of Si/Al ratios, ranging from Si/Al = 6.5 to pure silica materials. Al incorporation in the material has been characterised by different techniques and has evidenced a limit of about 6 Al/u.c. Increasing the Al content requires longer crystallisation times. This synthesis procedure exhibits nearly complete transformation of silica and alumina into crystalline zeolite and the system is highly stable at the synthesis temperature. A decrease in the amount of fluoride anions incorporated in the solid has also been observed when increasing the Al content until 4–5 Al/u.c. above which some TEA oxofluoroaluminate complexes can be present in the samples.

Characterisation of the materials by XRD, IR and ^{29}Si MAS NMR spectroscopies shows an increased resolution of the patterns when decreasing the Al content, this being due to the absence of connectivity defects and to the higher degree of order in the absence of Al. The samples show an enhanced stability upon calcination in static air compared to samples synthesised in basic medium. However, dealumination processes have been detected by IR and ^{27}Al MAS NMR spectroscopies with dealumination being more severe at higher Al contents. However, when calcination is carried out in an N_2 flow followed by air flow dealumination processes are reduced. Thermal analyses have shown differences for samples with high and low Al content which are related to decomposition of different species allowing a distinction to be made between TEA^+ compensating for framework Al and for fluoride anions.

The authors gratefully acknowledge the Spanish CICYT (MAT97-0372) for financial support.

References

1 E. M. Flanigen and R. L. Patton, *US Pat*., 4073865, 1978.
2 J. L. Guth, H. Kessler and R. Wey, *Stud. Surf. Sci. Catal*., 1986, **28**, 121.
3 J. L. Guth, H. Kessler, P. Caullet, J. Hazm, A. Merrouche and J. Patarin, in *Proc. Ninth Int. Zeolite Conf*., ed. R. von Ballmoos, J. B. Higgins and M. M. J. Treacy, Butterworth, Heinemann, 1993, p. 215.
4 H. Kessler, J. Patarin and C. Schott-Darie, *Stud. Surf. Sci. Catal*., 1994, **85**, 75.
5 M. A. Camblor, A. Corma and S. Valencia, *Chem. Commun*., 1996, 2365.
6 M. A. Camblor, A. Corma and L. A. Villaescusa, *Chem. Commun*., 1997, 749.
7 M. A. Camblor, A. Corma, P. Lightfoot, L. A. Villaescusa and P. A. Wright, *Angew. Chem., Int. Ed. Engl*., 1997, **36**, 2659.
8 R. L. Wadlinger, G. T. Kerr and E. J. Rosinski, *US Pat*. 3 308 069, 1967.
9 J. M. Newsam, M. M. J. Treacy, W. T. Koetsier and C. B. de Gruyter, *Proc. R. Soc. London A*, 1988, **420**, 375.
10 J. B. Higgins, R. B. La Pierre, J. L. Schlenker, A. C. Rohrman, J. D. Wood, G. T. Kerr and W. J. Rohrbaugh, *Zeolites*, 1988, **8**, 446.
11 J. C. van der Waal, M. S. Rigutto and H. van Bekkum, *J. Chem. Soc., Chem. Commun*., 1994, 1241.
12 M. A. Camblor, M. Costantini, A. Corma, L. Gilbert, P. Esteve, A. Martínez and S. Valencia, *Chem. Commun*., 1996, 1339.
13 R. J. Saxton, *US Pat*., 5453511, 1995.
14 R. J. Davis, Z. Liu, J. E. Tabora and W. S. Wieland, *Catal. Lett*., 1995, **34**, 101.
15 T. Blasco, M. A. Camblor, A. Corma, P. Esteve, A. Martínez, C. Prieto and S. Valencia, *Chem. Commun*., 1996, 2367.
16 S. Valencia, M. A. Camblor and A. Corma, *PCT WO Pat*., 97/33830, 1997.
17 T. Blasco, M. A. Camblor, A. Corma, P. Esteve, J. M. Guil, A. Martínez, J. A. Perdigón-Melón and S. Valencia, *J. Phys. Chem. B*, 1998, **102**, 75.
18 P. Caullet, J. Hazm, J. L. Guth, J. F. Joly, J. Lynch and F. Raatz, *Zeolites*, 1992, **12**, 240.
19 M. A. Camblor, A. Corma, S. Iborra, S. Miquel, J. Primo and S. Valencia, *J. Catal*., 1997, **172**, 76.
20 M. A. Camblor, A. Corma, A. Mifsud, J. Pérez-Pariente and S. Valencia, *Stud. Surf. Sci. Catal*., 1997, **105**, 341.
21 J. L. Guth and R. Wey, *Bull. Soc. Fr. Mineral. Cristallogr*., 1969, **92**, 105.
22 M. A. Camblor, A. Mifsud and J. Pérez-Pariente, *Zeolites*, 1991, **11**, 792.
23 J. L. Guth, H. Kessler, J. M. Higel, J. M. Lamblin, J. Patarin, A. Seive, J. M. Chezeau and R. Wey, in *Zeolite Synthesis*, ed. M. L. Occelli and H. Robson, *ACS Symp. Ser*., 1989, **398**, 176.
24 J. Dwyer, J. Zhao and D. Rawlence, in *Proc. Ninth Int. Zeolite Conf*., ed. R. von Ballmoos, J. B. Higgins and M. M. J. Treacy, Butterworth, Heinemann, 1993, p. 155.
25 M. A. Camblor, A. Corma and S. Valencia, manuscript in preparation.
26 M. A. Camblor, C. Corell, A. Corma, M. J. Díaz-Cabañas, S. Nicolopoulos, J. M. González-Calvet and M. Vallet-Regí, *Chem. Mater*., 1996, **8**, 2415.
27 H. Koller, R. F. Lobo, S. L. Burkett and M. E. Davis, *J. Phys. Chem*., 1995, **99**, 12 588.
28 P. Caullet, J. L. Guth and J. M. Lamblin, *Eur. J. Solid State Inorg. Chem*., 1991, **28**, 345.
29 M. Estermann, L. B. McCusker, C. Baerlocher, A. Merrouche and H. Kessler, *Nature*, 1991, **352**, 320.
30 A. Merrouche, J. Patarin, M. Soulard, H. Kessler and D. Anglerot, in *Synthesis of Microporous Materials*, *Molecular Sieves*, vol. 1, ed. M. L. Occelli and H. Robson, van Nostrand Reinhold, New York, 1992, p. 384.
31 P. A. Barrett, M. A. Camblor, A. Corma, R. H. Jones and L. A. Villaescusa, *J. Phys. Chem. B*, 1998, **102**, 4147.
32 G. van de Goor, C. C. Freyhardt and P. Behrens, *Z. Anorg. Allg. Chem*., 1995, **621**, 311.
33 H. Koller, A. Wölker, H. Eckert, C. Panz and P. Behrens, *Angew. Chem., Int. Ed. Engl*., 1997, **36**, 2823.
34 M. A. Camblor, A. Corma and S. Valencia, *Microporous Mesoporous Mater*., in press.
35 M. A. Camblor and J. Pérez-Pariente, *Zeolites*, 1991, **11**, 202.
36 J. H. De Boer, B. C. Lippens, B. G. Linsen, J. C. P. Broekhoff, A. van den Heavel and Th. V. Osinga, *J. Colloid. Interface. Sci*., 1966, **21**, 405.
37 E. Bourgeat-Lami, F. Fajula, D. Anglerot and T. Des Courieres, *Microporous Mater*., 1993, **1**, 237.
38 J. Pérez-Pariente, J. Sanz, V. Fornés and A. Corma, *J. Catal*., 1990, **124**, 217.
39 G. Engelhardt and D. Michel, *High Resolution Solid-State NMR of Silicates and Zeolites*, John Wiley and Sons, New York, 1987.
40 E. Bourgeat-Lami, P. Massiani, F. Di Renzo, P. Espiau, F. Fajula and T. Des Courières, *Appl. Catal*., 1991, **72**, 139.
41 S. A. Axon, K. Huddersman and J. Klinowsky, *Chem. Phys. Lett*., 1990, **172**, 398.
42 M. Soulard, S. Bilger, H. Kessler and J. L. Guth, *Zeolites*, 1987, **7**, 463.

Paper 8/04457K; *Received* 12*th June*, 1998